EES Solar

PAPER

View Article Online
View Journal | View Issue

Cite this: *EES Sol.*, 2025, **1**, 295

Long-term outdoor performance of a solar farm enabled by graphene-perovskite panels: investigating degradation mechanisms, dark storage recovery, and visual defects†

E. Spiliarotis,[a] G. Viskadouros,[ab] K. Rogdakis,[ac] S. Pescetelli,[d] A. Agresti,[d] N. Tzoganakis,[a] A. Di Carlo*[de] and E. Kymakis*[ac]

Outdoor performance monitoring of the emerging photovoltaic technologies, such as organic or perovskite solar modules, under real-life environmental conditions for an extended period will set the grounds for further technological maturity while revealing distinct characteristics compared to silicon or other commercial technologies. This study focuses on the long-term outdoor performance of a solar farm enabled by graphene-perovskite panels (S. Pescetelli, A. Agresti, G. Viskadouros *et al.*, *Nature Energy*, **7**, 597 (2022)). In this study, we investigated the solar farm's degradation mechanisms and a peculiar dark-storage recovery effect, as well as the light-soaking phenomenon that emerges after a dark-storage recovery process. The solar farm's performance was monitored over an extended period of time, and its performance was analyzed using a combination of electrical and optical characterization techniques. It was demonstrated that the key sources of solar farm degradation were exposure to high temperatures and solar irradiance while operating outdoors, as well as lamination failure due to aging that resulted in moisture and oxygen penetration. Notably, the visual defects observed in the perovskite modules during the performance monitoring period revealed severe effect of lamination failure on the graphene-perovskite solar farm performance degradation. The reported performance degradation was found to be partially restored after panels' dark storage indicating that both reversible and irreversible mechanisms are at play. A peculiar light-soaking phenomenon was also observed after the dark storage process, which led to partial performance recovery, indicating different behavioral trends after the dark storage of panels.

Received 26th March 2025
Accepted 28th March 2025

DOI: 10.1039/d5el00042d

rsc.li/EESSolar

Broader context

This study examines the long-term outdoor performance of a graphene-enabled perovskite solar farm, highlighting critical insights into the stability challenges and recovery mechanisms of the perovskite photovoltaics. Given the increasing demand for renewable energy, the development of efficient and stable perovskite-based solar technologies is essential for transitioning to sustainable energy systems. The study identifies the primary degradation factors—such as high temperatures, solar irradiance, and lamination failure—while demonstrating the potential for partial performance recovery through dark storage. The observed light soaking phenomenon also provides insights into the dynamic behaviour of perovskite solar panels. These findings underscore the importance of designing robust perovskite structures and improving encapsulation techniques to extend operational lifetimes. By correlating environmental impacts with performance changes, this research advances the understanding of perovskite photovoltaics' real-world reliability and contributes to the development of practical solutions for large-scale deployment. Ultimately, this study fosters progress toward achieving the economic and environmental benefits promised by next-generation solar technologies.

[a]*Department of Electrical & Computer Engineering, Hellenic Mediterranean University, Heraklion, GR71410, Crete, Greece. E-mail: kymakis@hmu.gr*

[b]*Department of Mineral Resources, Technical University of Crete, Chania, GR73100, Crete, Greece*

[c]*Institute of Emerging Technologies (i-EMERGE), University Research and Innovation Center, HMU, Heraklion, GR71410, Crete, Greece*

[d]*CHOSE—Centre for Hybrid and Organic Solar Energy, Electronic Engineering Department, University of Rome Tor Vergata, Rome, Italy. E-mail: aldo.dicarlo@cnr.it*

[e]*CNR-ISM – Istituto di Struttura della Materia del Consiglio Nazionale delle Ricerche, Rome, Italy*

† Electronic supplementary information (ESI) available. See DOI: https://doi.org/10.1039/d5el00042d

Introduction

Perovskite solar cells have garnered significant scientific attention as an emerging photovoltaic technology because of their promising characteristics, such as unique optoelectronic properties, high power conversion efficiency (PCE),[1–3] low-cost and facile, solution-based fabrication at low temperatures, and mechanical flexibility.[4] Research on perovskite solar cells (PSCs) and modules has focused on improving the device performance and durability,[5] while testing the devices using

specific measurement protocols[6] under both indoor[7] and outdoor[8–12] conditions. Notably promising path toward increasing the PCE further is to develop various tandem structures by combining the PSCs with silicon or other photovoltaic technologies, opening the path for more efficient panels that could lead to cheaper electricity.[13,14] Efforts have focused on optimizing the composition of perovskite materials, interface engineering, device architectures, and fabrication techniques to achieve higher efficiencies.[15,16] Even though the PSCs have achieved a certified PCE with values up to 26.1% (USTC)[17] reported in 2023, thus outperforming conventional thin film solar cells such as crystalline Si, CIGS, and CdTe, more fundamental research is still needed at both material and device levels toward commercialization.[18]

Research has focused on improving the stability and durability of perovskite solar cells and modules. Perovskite technology is known to be susceptible to external environmental factors such as oxygen,[19] moisture,[20,21] temperature,[20,22–25] as well as exposure to high solar irradiance[26] and specifically the ultraviolet (UV) spectrum that can induce photochemical reactions and degrade the organic components of the device.[27] These environmental factors affect the perovskite layers differently, resulting in a reduction in their PCE and more importantly, in their lifetime stability.[18,28–30] Specifically, moisture ingress can cause perovskite materials to degrade, resulting in reduced device performance,[21] increased hysteresis, and, eventually, device failure. Exposure to intense sunlight and prolonged light exposure can lead to the formation of phase segregation,[31] defects, trap states, and photo-induced degradation in perovskite materials, resulting in reduced device performance and stability. High temperatures can accelerate degradation processes such as ion migration,[32] decomposition of organic components, and phase transitions in perovskite materials, leading to device instability and reduced efficiency. Thermal management strategies such as heat sinks and thermal pastes are employed to mitigate the effects of temperature on perovskite solar cells. Encapsulation techniques, UV-blocking layers, and interface engineering have also been explored to mitigate degradation mechanisms and enhance long-term stability by minimizing the effects of light exposure. The demonstration of long-term stability is still a significant challenge that this technology must overcome.[5,33]

In some examples, continuous light illumination or light soaking can enhance the performance through light-induced structural dynamics that locally relax strain, lower energetic barriers, or decrease the surface accumulation of photogenerated charge carriers at the electrode interfaces, thus improving the open circuit voltage and fill factor.[34,35] There are various sources of degradation in PSC reported in the literature,[33] such as migration of cations,[36] non-radiative recombination processes,[37,38] columnar intergrains and defective spots in the perovskite bulk,[39] the nature of the hole transport layer,[10,40] or the perovskite stoichiometry.[41] Some studies have indicated partial recovery of some electrical properties when devices are stored in the dark for some period.[9,18,31] Some reports even stated that recovery occurs during nighttime hours,[18] urging for a systematic investigation of the operation conditions on the degradation behavior of PSC, being either reversible or permanent.[42]

Most of the reported studies on PSC have been implemented indoors by accelerated International Summit on Organic Photovoltaic Stability (ISOS) stability tests to simulate the real-life exposure conditions of photovoltaic cells in the field and thus be able to estimate their lifetime.[26] Initial reports suggested that the most reliable way to investigate PSC stability is under 1 sun illumination, preferably at the maximum power point (MPP), and both under room and elevated temperatures.[43,44] However, more accurate conclusions were derived by simulated ambient conditions based on real temperature and irradiance data, revealing that only a low decrease in efficiency with elevated temperature and low light intensity was observed, maintaining almost optimum values for ambient conditions.[40] Therefore, long-term stability measurements outdoors are necessary to identify the real-life performance of the technology that cannot be captured with solar simulators.[8]

In field measurements, during the day, there are gradual fluctuations in the intensity of solar irradiance and temperature[45] in contrast to the ideal lab conditions, where continuous illumination of 1 sun is provided. In addition, the overall exposure time and solar irradiance intensity are lower during cloudy days, whereas the phenomena that occur during night time, such as recovery effects on electrical characteristics,[23,44,46] cannot be simulated. Despite several studies having investigated the short-term lifetime of PSCs in outdoor conditions,[9,30,36,42,45,47,48] data are still required on the long-term outdoor stability, especially when the modules exhibit low PCE levels; thus, a detailed investigation of the degradation mechanisms can take place. Most of the outdoor evaluation is based on PSC, and only a few studies have been demonstrated on modules[47] or panels[8] level, pinpointing the crucial role of perovskite additives, HTL selection, and perovskite stoichiometry in partially reversible degradation effects by dark storage.[49] Notably, it was recently reported that the presence of various degradation patterns for different PSCs implies that accelerated aging with constant light experiment is no ''worst-case scenario'' and thus cannot replace the light cycling[50] test nor can it reproduce the real-world scenarios.[10]

The authors of the present study have fabricated the world's first solar farm based on graphene-enabled perovskite panels, while the outdoor stability of the system was investigated for a period of ~5000 hours of exposure. In Fig. 1, the generated power over the entire lifetime of the solar farm is presented, indicating that an abrupt reduction in the generated power from ~200 W down to ~90 W is observed in March 2021. This period coincides with an obvious failure of some panels' lamination (Fig. 1) that led to a penetration of moisture (when high levels of humidity and rainfall were recorded). The visual inspection of the panels indicated that only some panels suffered from this lamination issue, whereas the encapsulation of the modules prevented deeper moisture penetration at the cell level. In the current follow-up study, long-term performance monitoring of both the solar farm as a whole and of each panel from 3/2021 to 10/2022 is presented. Moreover, various degradation mechanisms were carefully investigated, and the effects

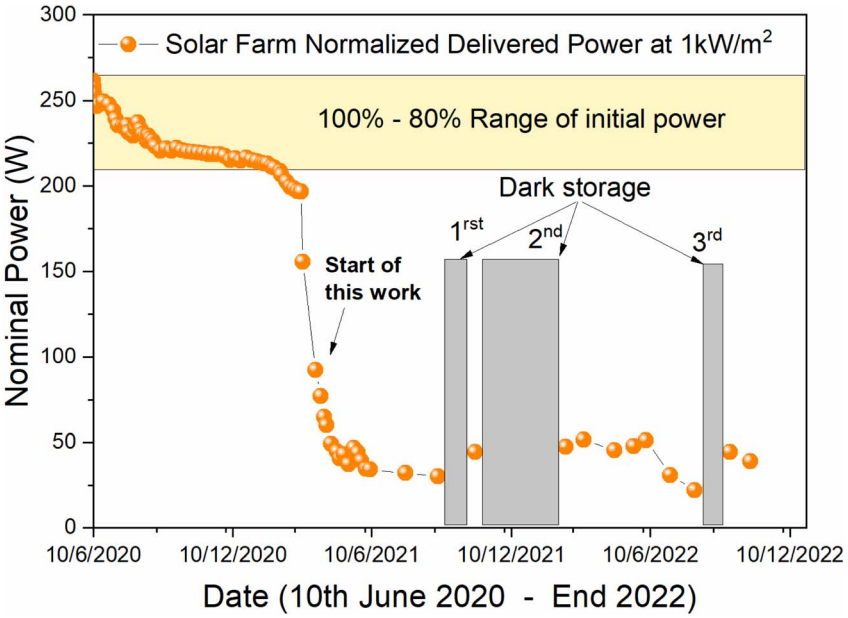

Fig. 1 Evolution of solar farm nominal power for the period 06/2020 till 12/2022.

of dark storage and light soaking on panel performance were studied. The dark storage of the panels was found to have a beneficial effect on the output power of the panels.

The detailed set of measurements implemented in this study allows a comprehensive understanding of the degradation mechanisms, providing insights into designing stable[51] and efficient cells, modules, panels and solar farms based on perovskite technology. Feedback from outdoor monitoring will also allow for the optimization of panel manufacturing processes, such as lamination techniques,[52] towards enhanced endurance against severe real life environmental conditions. Overall, it is necessary to establish specific measurement protocols that can be applied commonly in outdoor conditions, allowing various labs to produce comparable and reproducible results.

Methodology

Solar farm Graphene Perovskite panels interconnection and solar farm assembly

All the experiments presented in this study were conducted at the HMU's solar farm located in Crete consisting of 9 Graphene Perovskite (GRAPE) panels, as reported in our previous study.[8] Each panel contained 40 GRAPE modules (5 in parallel, connected in rows of 8 in series). The modules were fabricated using the following cell stack in which 2D materials were integrated at various places across the device structure: glass-fluorine doped tin oxide (FTO)-compact TiO_2 + graphene ($cTiO_2$ + G)/mesoporous TiO_2 + graphene ($mTiO_2$ + G)/mixed-cation perovskite/$fMoS_2$/poly(triaryl amine) (PTAA)/Au. Extended details on material formulation and characterization, as well as manufacturing processes, can be found in ref. 8. Finally, for the realization of the solar farm, all panels were connected in parallel to allow accurate performance comparisons between measurements. Due to the parallel connection, the open circuit voltage (V_{OC}) of the solar farm was the nominal V_{OC} output of the panels and the current production was the sum of all 9 panels. In this configuration, current production was maximized, thereby improving the efficiency of the battery charging system.

Dark storage

During this study, the panels of the solar farm were stored indoors at different time periods and for different time intervals to determine whether recovery effects on the electrical characteristics occurred and how these effects affected the panel performance. The applied dark storage (DS) methodology followed the ISOS-D-1 protocol,[6] which involved storing the GRAPE panels in a completely dark environment at ambient air temperature, relative humidity, and environmental conditions.

I–V characterization of solar farm and monitoring methodology

The electrical characterization of the solar farm was performed by measuring forward *I–V* (short circuit current to open circuit voltage) characteristics during the day. The measurements were taken every 50 W m^{-2} (0.05 sun) change in solar irradiance on sunny days using the electronic load PV-blocks (by EKO Instruments). Comparisons were made between the morning and afternoon values at the same irradiance levels, as well as over time for the period in which the panels were outdoors. The transition between morning and afternoon values was defined as the time of day when the solar irradiance value peaked and began to descend. Outdoor stability monitoring was performed according to the ISOS-O-2 protocol.[6] The goal was to observe the differences in the solar farm behavior at distinct performance periods, namely when degradation was reported, after the dark-

storage enabled partial recovery (DS) of the panels, and then each month after the recovery had occurred.

Light soaking methodology

The light-soaking experiments were performed to investigate the dependence of various electrical characteristics, such as V_{oc} (open circuit voltage), I_{sc} (short circuit current), P_{max} (maximum power), and FF (fill factor), on light illumination. The forward *I–V* measurements were performed using the PV-blocks electronic load (by EKO Instruments) at 1-minute intervals until the electrical characteristics were stabilized. After ensuring that all the electrical values had the same behavior during light soaking, the rest of the light-soaking experiments were performed by continuously measuring only the V_{oc} at 1-minute intervals.

Because a light-soaking protocol (such as ISOS-L) is not available for outdoor measurements, the following methodology was proposed and used for the experiments: the GRAPE panels were initially exposed to sunlight under ambient temperature, relative humidity, and outdoor environmental conditions. The characterization light source was sunlight on a clear day, and the load used was at OC (open circuit). The experiments were conducted during midday to maintain a nearly stable solar irradiance of 1000 ± 10 W m^{-2} for a sufficiently long period to ensure consistency. To minimize any changes in panel temperature and relative humidity during measurements, the GRAPE panels were simply covered to block light illumination; however, they were still exposed to the surrounding environmental conditions.

Environmental conditions monitoring

Environmental conditions were monitored during all experiments, and their correlation with the outdoor performance of the GRAPE panels (ESI Fig. 1 and 2†). The weather station used to monitor the environmental conditions consisted of a data logger (Campbell Scientific CR1000) and several weather parameter sensors, including air and panel temperature, relative humidity, wind speed/direction, and a pyranometer for solar irradiance.

Visual inspection

A visual inspection approach was used to track any visual defects or changes in the panels over time. Photos[53] were taken during the panels' outdoor lifetime, and differences between them were compared to identify any visual changes. The visual monitoring also aimed to observe vulnerable spots on the panel due to moisture penetration resulting from lamination failure and to investigate how this effect affected module performance as the moisture penetration progressed.

Results and discussion

Visual inspection of GRAPE panels

A visual inspection process was conducted throughout the lifetime of the GRAPE panels measured under outdoor conditions in alignment with other outdoor test protocols for perovskite PV panels.[53] This involved the periodic capture of photos that allowed for observing visible signs of degradation, such as module discoloration, and to identify the most vulnerable areas of the panels to moisture and oxygen penetration, which are known to have a destructive effect on PSCs.[54,55]

The comparison of the captured images revealed various visual defects that could be attributed to different factors. Some defects were linked to imperfections that occurred during the fabrication process, while others were a result of degradation factors like prolonged irradiation and elevated temperature over time.[56,57] In addition, some defects were associated with

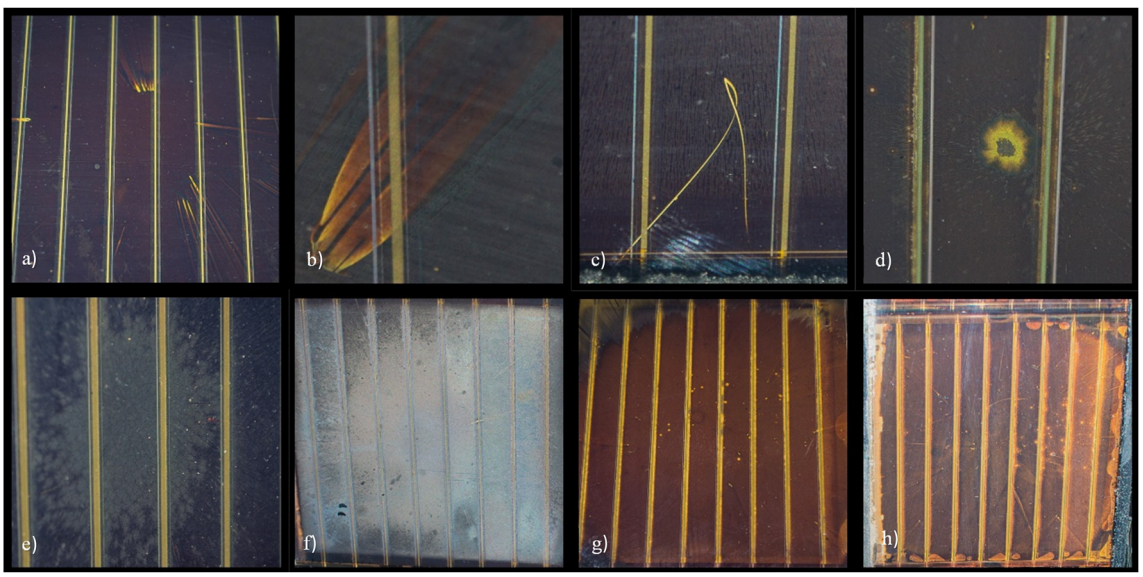

Fig. 2 GRAPE panels visual defects (a) and (b) flairs, (c) cracks, (d) holes, regions suffered by (e) oxygen penetration, and (f)–(h) moisture penetration in the panel module.

moisture and oxygen penetration from vulnerable spots where panel lamination failed.

The aggregated results of these visual degradation defects are presented in Fig. 2, including the following categories: (1) flairs, (2) microcracks, (3) appearance of cell holes, and (4) regions suffering from moisture and oxygen penetration.

However, some panels did not exhibit lamination failure and demonstrated resilience against outdoor conditions, retaining their characteristics at a higher rate. Fig. 3 shows representative examples of a less discolored panel (panel #7) and a more discolored panel (panel #9 and panel #3), respectively.

Fig. 3 shows a side-by-side comparison of the three panels, indicating two panels that experienced moisture penetration through different pathways (panel #9 and panel #3) and one panel with better structural and morphological stability over time due to a more robust lamination. One panel demonstrates lamination failure on the sides (panel #3), the other within the junction box, which is in the center of the back side (see ESI Fig. 8†) of the panel, (panel #9), and another panel (panel #7) showing only minor discoloration over time that exhibited remarkable endurance in outdoor conditions.[58]

In cases where lamination failed on the side of the panel (panel #3), it is evident that moisture and oxygen penetration gradually affected multiple modules within the panel. In contrast, moisture and oxygen penetration from the junction box occurred at a slower rate, resulting in a different form of discoloration (panel #9). This difference can be attributed to the fact that the back of the panel is more protected from environmental factors, such as rain, compared to the edges of the panel.

Effect of parallel connection of GRAPE-panel-based solar farm

Although there are some published studies on the stability of perovskite photovoltaics under outdoor conditions,[10,12,59] they all refer to characterization measurements performed on single cells and not on a combination of cells integrated into modules or even multiple modules. However, the degradation mechanisms induced by the system configuration are also relevant in PV plants.[60]

As mentioned in the methodology, all panels were connected in parallel to maximize the current production and thus improve the efficiency of the battery charging system. However, each panel exhibited a different degradation rate throughout its lifetime, resulting in voltage mismatch between panels. One approach to overcome this voltage mismatch would be to change the configuration of the panel's connections, *i.e.*, to connect panels with lower voltages in series and then in parallel with others to reduce this effect. However, this would make previous solar farm measurements inaccurate.

It is widely known in the literature that voltage mismatch across a photovoltaic module results in a built-in electric field that can cause various forms of degradation.[60,61] This effect is inevitable in perovskite photovoltaics because of the different degradation rates expected in individual samples (cells, modules, panels) integrated, affecting the local V_{oc} of each cell or module. Thus, the built-in electric field originating from the voltage mismatch in the perovskite modules can be described as a DC bias. It is also known that external DC biasing is beneficial for a short period and is also used as a preconditioning method before electrical characterization for PSC[62,63] (pre-bias step); however, it is not ideal for long periods of time or for values higher than the V_{oc} of the sample.[64,65]

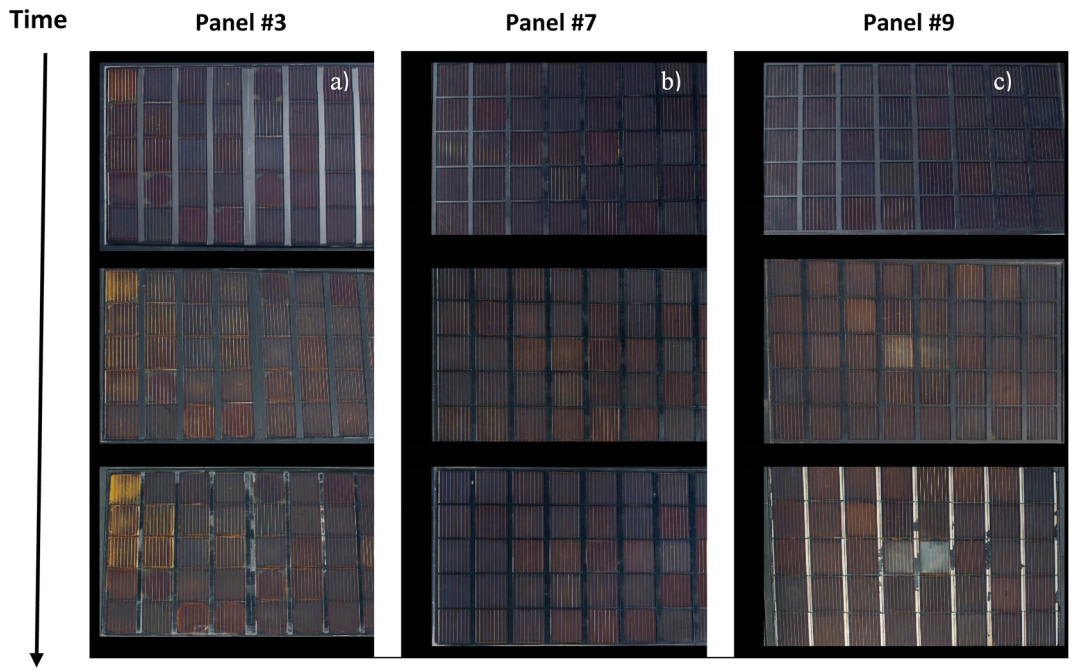

Fig. 3 Side-by-side comparison of 3 GRAPE panels: (a) GRAPE panel #3, (b) GRAPE panel #7, and (c) GRAPE panel #9. The 1st row shows GRAPE panels before the period of lamination failure, the 2nd row shows the period of the lamination failure and the 3rd row after the lamination failure and the different pathways of moisture and oxygen penetration in the panels.

Table S1 (ESI)† shows the V_{oc} values of each panel and the solar farm as a system for each month after the 3-month DS period. To ensure that this comparison is accurate, the measurements were conducted midday at the peak of solar irradiance in each month, when solar irradiance is stable, so the changes due to fluctuations in irradiance can be ruled out. The total V_{oc} output of the solar farm lies between the values of the individual panels and is not close to the expected minimum. If the panels had no losses, we would theoretically expect them to have the lowest voltage, as is the case with the parallel connection of the current sources. We can assume that this behavior can be attributed to different levels of degradation leading to different electrical equivalent circuits than expected for parallel connection. These internal parasitic connections across various modules of each panel could explain the apparent overall solar farm voltage being close to the average value of independent panels. It should be noted that after this DS period, the total V_{oc} value of the solar farm is very close to the average of the V_{oc} values of the individual panels (difference < 5%) and deviates quite strongly from the V_{oc} value of the panel with the lowest value (difference > 30%). We noticed that the V_{oc} value of the solar farm gets even closer to the average value of the 9 panels V_{oc} and even reaches deviations of <1% in July 2022, after the gradual decrease in the V_{oc} values of the individual panels reported during monthly measurements.[66]

Electrical characteristics recovery in GRAPE panels enabled by DS

In the following, we investigate the long-term photovoltaic performance of GRAPE panels under real outdoor conditions between 3/2021 and 10/2022, which corresponds to the T_{40} point of solar farm operation (Fig. 4 and ref. 8) and beyond (T_{40} is defined as the period when the efficiency of the solar farm was reduced to 40% of the initial value). Data from the performance monitoring from 06/2020 to 06/2021 have been published in ref. 8. During the first 10 months of the solar farm operation, a slow decrease in the nominal power was observed, indicating a T_{80} of 5832 h (at ~month 8), which was attributed to intrinsic perovskite degradation mechanisms.[54,55] However,

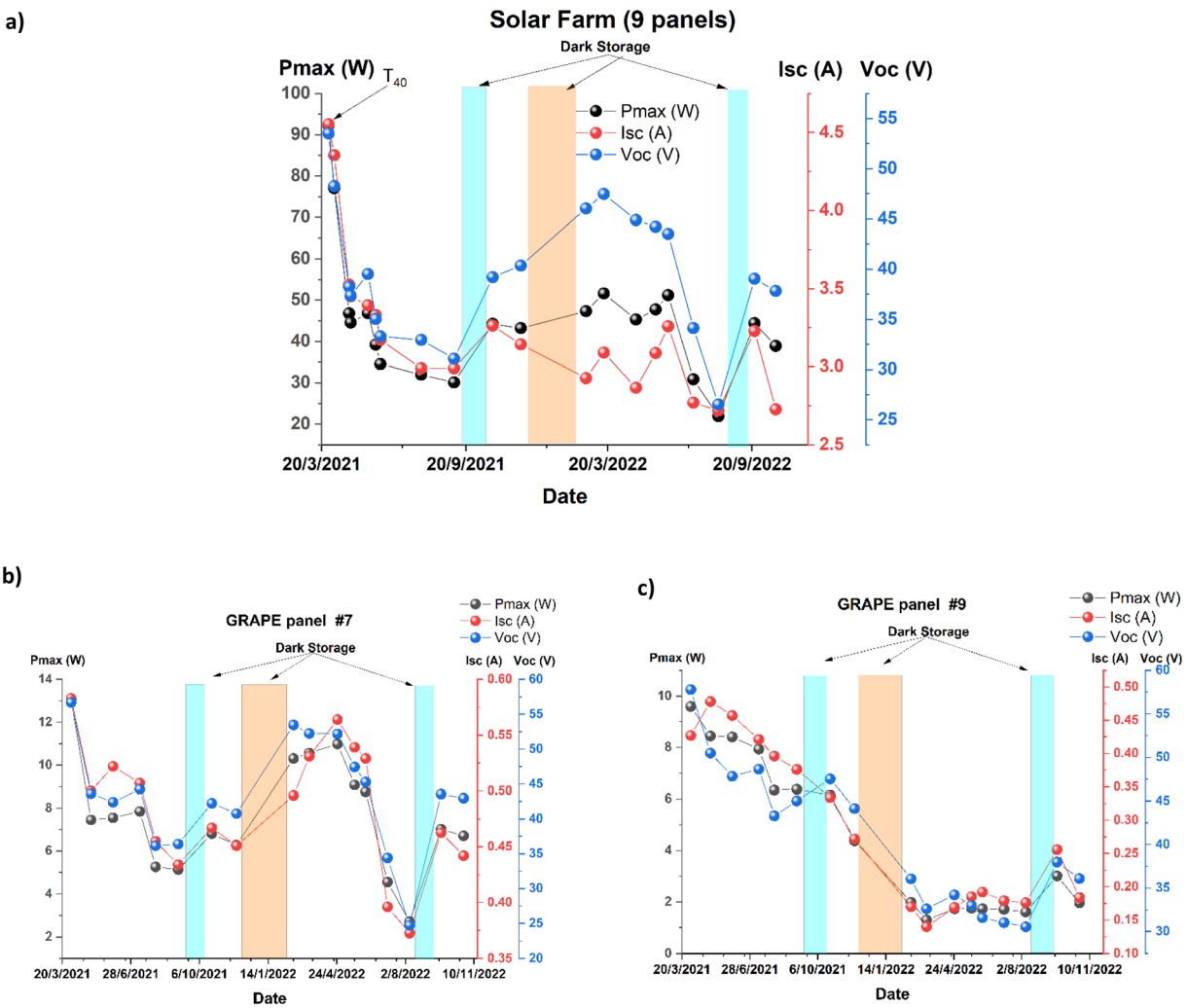

Fig. 4 Electrical parameters (P_{max}, I_{sc}, and V_{oc}) extracted from the I–V characteristics of (a) solar farm, (b) GRAPE panel #7, and (c) GRAPE panel #9 for the period 2021–2022. In graphs a, b and c, dark storage periods are highlighted with (a) cyan (1 month DS period applied twice), (b) orange (3 month DS period applied once).

a notable abrupt reduction in the electrical properties of both the individual solar panels and the entire solar farm was observed after the first 10 months of the solar farm operation, which is likely related to an extrinsic degradation mechanism. This period coincides with the start of the spring period.

Fig. 4 illustrates the changes in V_{oc}, I_{sc} and P_{max} for individual representative panels that exhibit different degradation levels and the entire solar farm before and after the DS processes. Two different dark storage periods are tested in Fig. 4, either 1 month (boxes with cyan color) or 3 months (boxes with orange color).

As mentioned in the previous section, moisture ingress in the panels upon lamination failure is the dominant degradation factor. The degradation can be attributed to exposure to elevated temperatures and prolonged sunlight illumination, especially after the end of winter when longer daylight hours are expected with high irradiance levels (see Fig. 5). This suggests that the GRAPE panels may experience a seasonal degradation rate that reduces their electrical performance. Extrinsic and intrinsic perovskite degradation mechanisms are also involved.

Even panels with lamination issues can recover their performance after DS as long as the module encapsulation remains undamaged,[67] preventing moisture penetration that could degrade the perovskite layer. Therefore, the daily deterioration during these months surpassed the partial recovery that occurred during the night,[18] leading to a gradual decrease in electrical properties over this period. For the non-reversible degradation process, two criteria should be fulfilled: panel lamination failure and local cell encapsulation failure leading to perovskite degradation due to environmental conditions.

After the panels were stored indoors for approximately one month (from 06/09/2021 to 23/10/2021) – first cyan column bar in Fig. 4 – a significantly higher recovery rate of the electrical properties was observed, as opposed to the day–night cycle,[18] where a partial and weak recovery has been demonstrated in literature in fresh, non-degraded perovskite cells.

For a detailed quantitative analysis, Table S2† presents the percentage (%) increase or decrease in the electrical characteristics of each panel observed during each dark storage (DS) period. Moreover, Fig. S7 in ESI† presents various histograms of the ±% increase/decrease of each electrical parameter (P_{max}, I_{sc}, and V_{oc}) during each DS period for the nine panels of the solar farm. The average values of each figure of merit of all 9 panels are also presented in their corresponding Fig. S7.† It is evident from Fig. 4 and S7† that not all panels followed the same trend after applying each DS process; therefore, evaluating the percentage increase or decrease in the electrical characteristics of each panel as presented in Table S2† could be more valid. The average P_{max} values of the nine panels exhibit an increase of over 12% after dark storage, regardless of storage duration (one or three months). A similar monotonic behavior is reported in V_{oc} values after the corresponding DS processes, reaching an enhancement by 15%, 14% and 44% after DS 1,2 and 3, respectively (Fig. S7 and Table S2†). After DS 3, the highest percentage of performance recovery was reported due to lamination problems in some panels (*e.g.*, panel #3, panel #9). The parameter that is most affected by the various degradation levels of the panels is I_{sc}, where percentage fluctuations are observed after the DS periods.

Panels that exhibited less discoloration showed greater recovery (panel #7) and demonstrated performances comparable to those of the previous year. On the other hand, panels with more discoloration exhibited a lower recovery rate or even a reduction in their electrical characteristics after the DS periods (panel #9). The results for the remaining grape panels for the period 2021–2022 are presented in ESI Fig. 4.†

After a 3-month dark storage period indoors, the panels were reinstalled in their initial mounting system and monitored continuously. Fig. 4 shows that panel #7 exhibited an initial partial recovery even after the 3-month DS, which was not the case for panels such as panel #9, which exhibited a performance degradation. Interestingly, the panels that did not show recovery during the initial dark storage period exhibited temporal improvement upon exposure to sunlight for some period before starting to decline again.

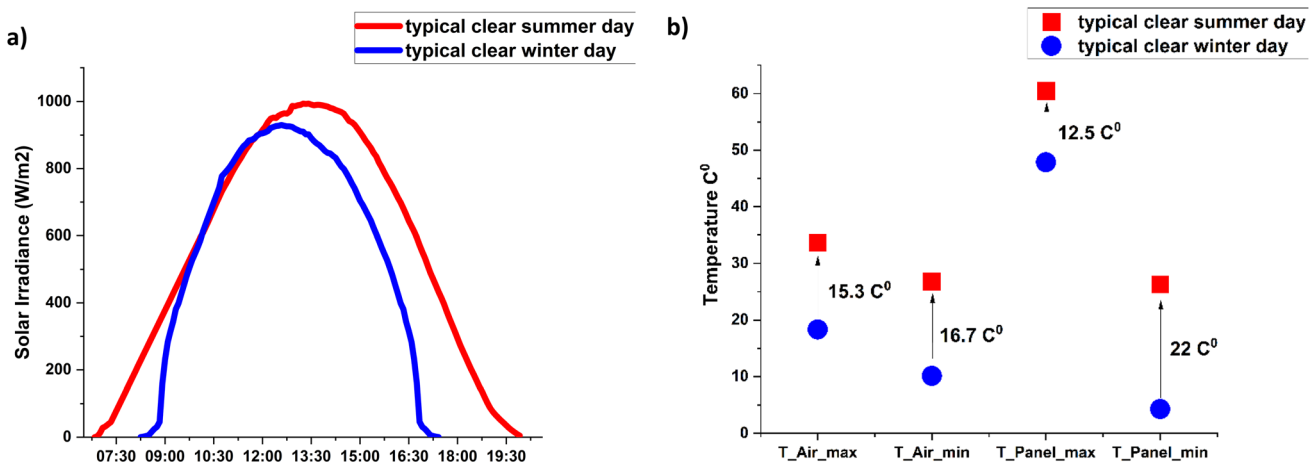

Fig. 5 Comparison between the winter and summer clear days of (a) different irradiation levels and duration. (b) Comparison of maximum air and panel temperature.

The solar farm as a whole demonstrated an average degradation/regeneration rate. This is a result of the parallel connection of the panels, where panels with higher initial voltage (V_{oc}) tend to bias panels with lower initial V_{oc} by adding their current values together.

Further analysis of the electrical characteristics of each panel, along with continuous monthly measurements and recording of these values, revealed an additional phenomenon. For panels that did not experience recovery but instead exhibited a decrease in electrical properties after the first and second dark storage periods (see behavior of panel 9 as representative example), an increase in their electrical characteristics was observed as soon as they were reinstalled on their mountings after the 3rd DS. This observation aligns with findings in the literature on perovskite photovoltaics,[36] which categorizes the degradation of PSC into two different phases, each based on a different mechanism inherent to the perovskite layer or extrinsic originating from lamination and encapsulation failure. In the first period, a reversible degradation occurs during day/night cycles, which is the behavior observed before the T_{80} period; thus, the lamination and encapsulation of the panels are not severely degraded. This intrinsic degradation can be attributed to the formation of metastable defects or reversible ion redistribution under light illumination or electric bias. The second period emerges after T_{50} when the GRAPE panels exhibit distinct performance recovery dynamics. In this phase, the FF (fill factor) and I_{SC} (short-circuit current) rapidly increase with extended light illuminations (Fig. 4b). The formation of a charge extraction barrier induced by de-trapping interfacial shallow traps when light is switched off could be the mechanism behind this behavior.[36] During this phase, which occurs after the PCE has dropped to 20–50% of the initial values, performance recovery is possible but takes longer than a single night, making it non-reversible within the day–night cycle.[36] Ion-vacancy recombination process enabled by photo-induced halide redistribution could lead to current modulation upon illumination. Moreover, light illumination can lead to an overall current enhancement attributed to a photogenerated electric field that lowers Schottky barriers driven by trapped photogenerated holes or vacancies. During nighttime, charge carriers are released from these traps, resulting in the formation of an interfacial charge extraction barrier.[36]

Furthermore, we observed that depending on the position of the discolored modules within certain panels, no overall recovery of the I_{SC} was observed. This is due to the in-series connection of the eight modules composing each string; thus, if one module fails, the entire series is affected, directly impacting the total current generation through the string of the panel.

Finally, as shown in Fig. 4, after T_{50}, all panels experienced a significant decrease in their electrical properties during the summer, even after the DS periods, confirming the presence of a seasonal degradation rate for the GRAPE panels.

The panels were stored once again for approximately one month (from 10/08/2022 to 20/09/2022) (cyan column bar in Fig. 4). During this period, the panels exhibited a recovery of their electrical characteristics, although to a lesser extent. However, the modules that suffered from moisture insertion resulted in a perovskite layer with clear visual degradation and were unable to operate again, giving a minimum contribution of current in the connected series.

Note that panel #7 demonstrated a substantial power recovery once again, and the subsequent decrease in the following month was smaller compared to panel #9. Although panel #9 exhibited a recovery, it shows significant degradation during the following month of operation. These observations suggest that the panels that initially depicted an abrupt degradation experienced a faster recovery after the DS process.

The percentage increase or decrease in the electrical characteristics of each panel during each dark storage (DS) period is provided in Table 2 of the ESI.†

Light soaking phenomenon (LSP) in GRAPE solar farm

Another phenomenon that was investigated in this study consists of the light-soaking effect that occurs when the perovskite panels are exposed to sunlight. DS observed in GRAPE panels should be related to LSP and the associated light-induced carriers and ions migration across the perovskite bulk and potential trapping effects at relevant interfaces, with a direct impact on V_{oc} values on cell, module and panel levels that leads to voltage mismatch effects observed in the current study.

LSP induces drastic changes in the optoelectronic properties under illumination and is usually observed in hybrid perovskite materials.[68] LSP should be avoided to achieve long-term operational stability in perovskite devices.

PSCs often exhibit light-soaking behavior under illumination conditions, which can gradually affect device performance. Experimental studies [35,68–70] have shown that light soaking is associated with interfaces between electrodes and active layers in planar-heterojunction PSCs.[71] In general, the light soaking and hysteresis effects can be attributed to polarization effects caused by lattice distortions, carrier trapping/interception, ion migration[32,72] and photoinduced halide segregation (PIHS) in PSCs.[31,44,58,73]

The light soaking phenomenon has been observed in PSCs having different device structures, which raises concerns about the instability of the power output of PSCs. Nonetheless, the severity of the light-soaking phenomenon varies from laboratory to laboratory and has been the subject of intense discussions on the underlying mechanism.

One of the proposed mechanisms is based on trap-filling/detrapping,[74] where traps are filled under light illumination. The long timescale observed in this process leads to controversial discussions about the location, properties of the trap states,[75,76] and the role of light-generated charge carriers and mobile ions in the trap-filling process.[74] The second mechanism is based on a type of doping where mobile ions drift to the opposite electrode under a photogenerated electric field, causing p- and n-doping at the anode and cathode, respectively. The latter mechanism does not consider the role of traps in light-soaking. In addition, mobile carriers and their drifting directions are still debated. The third mechanism proposed to

explain the light-soaking effect considers variations in the crystal structure of the perovskite due to the rotation/alignment of the methylammonium cations under light and bias. Nonetheless, drawing conclusions from these studies is difficult because of the different device structures and perovskite morphologies obtained in numerous research laboratories.[68] Moreover, optical measurements have revealed that carrier trapping (bulk trapping) strongly affects the photoconductivity response and consequently generates photocurrent hysteresis phenomena. In addition, electrochemical impedance spectroscopy (EIS) and ultraviolet photoemission spectroscopy (UPS) studies suggest that energy level alignment and trap filling can also lead to "light soaking" behavior.[77,78]

During LSP, changes in the electrical parameters of the panels were also observed. For the phenomenon of light soaking, comparative experiments were conducted to determine whether it is possible to distinguish the degradation of perovskite panels from their different origins.

For both panels (panels #7 and #2), the first measurements (measured at 4/21 and 8/21) show a typical behavior expected from the literature at this degradation state:[68,69] as soon as the panels are exposed to light, the V_{oc} exhibits an upward trend. However, just after the 3-month DS period, all panels exhibited different behaviors. When exposed to sunlight, the electrical properties start at a higher voltage than before partial recovery and then decrease towards stabilization. As shown in Table S3,† panel #2 exhibited an increase in average V_{oc} measured during LSP from ~36 V to ~53 V, panel #7 an increase from ~35 V to ~49 V and the average overall panels is a recovery over 15% for V_{oc} between 08/21 and 02/22, including 1 and 3-month DS periods.

After this different behavioral trend had been observed on 2/22, the same experiment was carried out for a second time on 3/22 without any measurements or light exposure between these dates. The results show identical behavior to the experiment of 2/22 for all panels during the LS in terms of the open circuit voltage, with an average variation in all GRAPE panels of approximately 0.4%. This is due to the lack of deterioration under illumination because the experimental measurements stress the panels, accelerating the reduction in their electrical properties due to LID.

To investigate any changes in this behavior, V_{oc} measurements were conducted each month after the 3-month DS. Fig. 6 shows the behavior of the V_{oc} for the solar farm, with panel #7 and panel #2 as representative examples. Results for the rest of the panels can be found in ESI Fig. 5.†

After re-installation of the mounting system, the LSP measurements indicate a gradual decrease in electrical performance during measurements and the exposure to high sunlight illumination, as mentioned earlier. The behavior during LSP gradually changes each month after the DS until it returns, from month 5/22 to its pre-DS recovery period state, *i.e.*, the values of electrical properties start increasing until they stabilize, as soon as the panels are exposed to solar irradiation for some time. Although V_{oc} increased for all panels after the DS, more degraded panels were observed (ESI Fig. 5† panel #3). Requiring more time to change the behavioral trend to the "pre-DS" upward trend.

It is worth noting that during the LSP, minor fluctuations in solar irradiance were reported (less than 15–20 W m^{-2}), thus they do not affect the electrical properties of the panels. However, after LSP application, a strongly solar irradiance-dependent behavior was observed for all electrical properties.

To ensure that all electrical properties followed the behavior of V_{oc}, a series of experiments was conducted, where forward *I–V* characterization curves were recorded, as described in the methodology section. These experiments were implemented for the entire solar farm and each panel to determine the correlation between the suppressed electrical properties of the panels

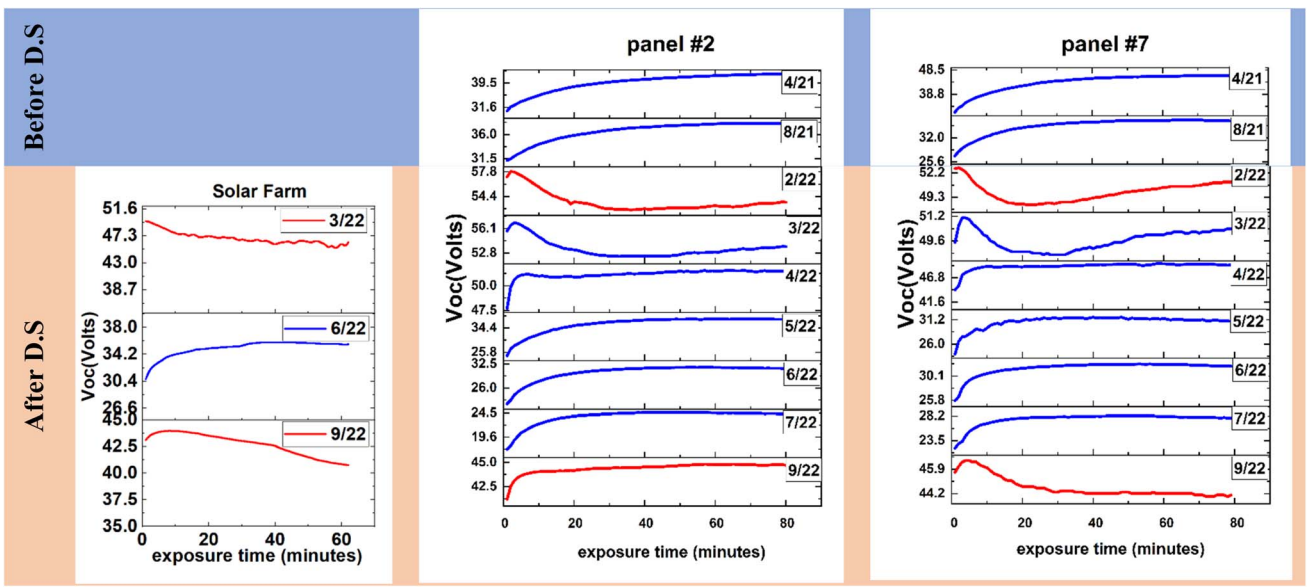

Fig. 6 Light soaking effect behavior change before (4/21 and 8/21) and after the 3-month dark storage (DS) period (2/22) for the solar farm, panel #7, and panel #2, for each month until 9/22. The red color highlights the measurements immediately after the DS periods (2/22 and 9/22).

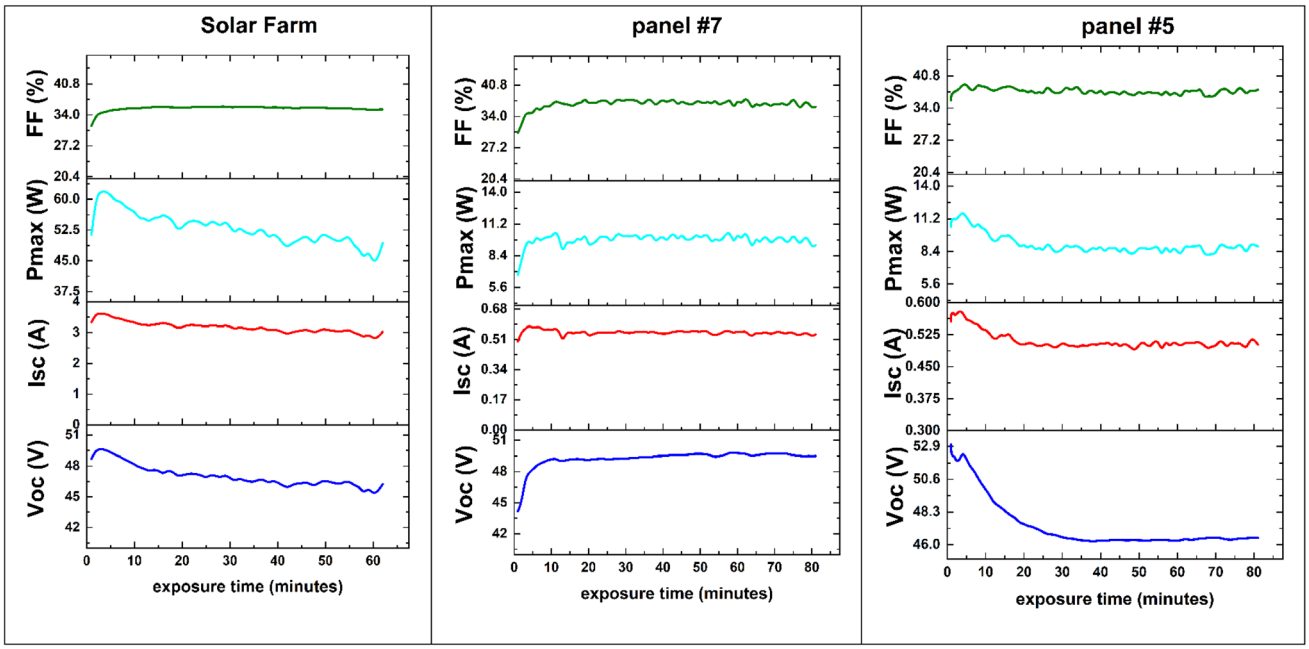

Fig. 7 Electrical characteristics during the light soaking effect for the GRAPE solar farm, panel #7 and panel #5.

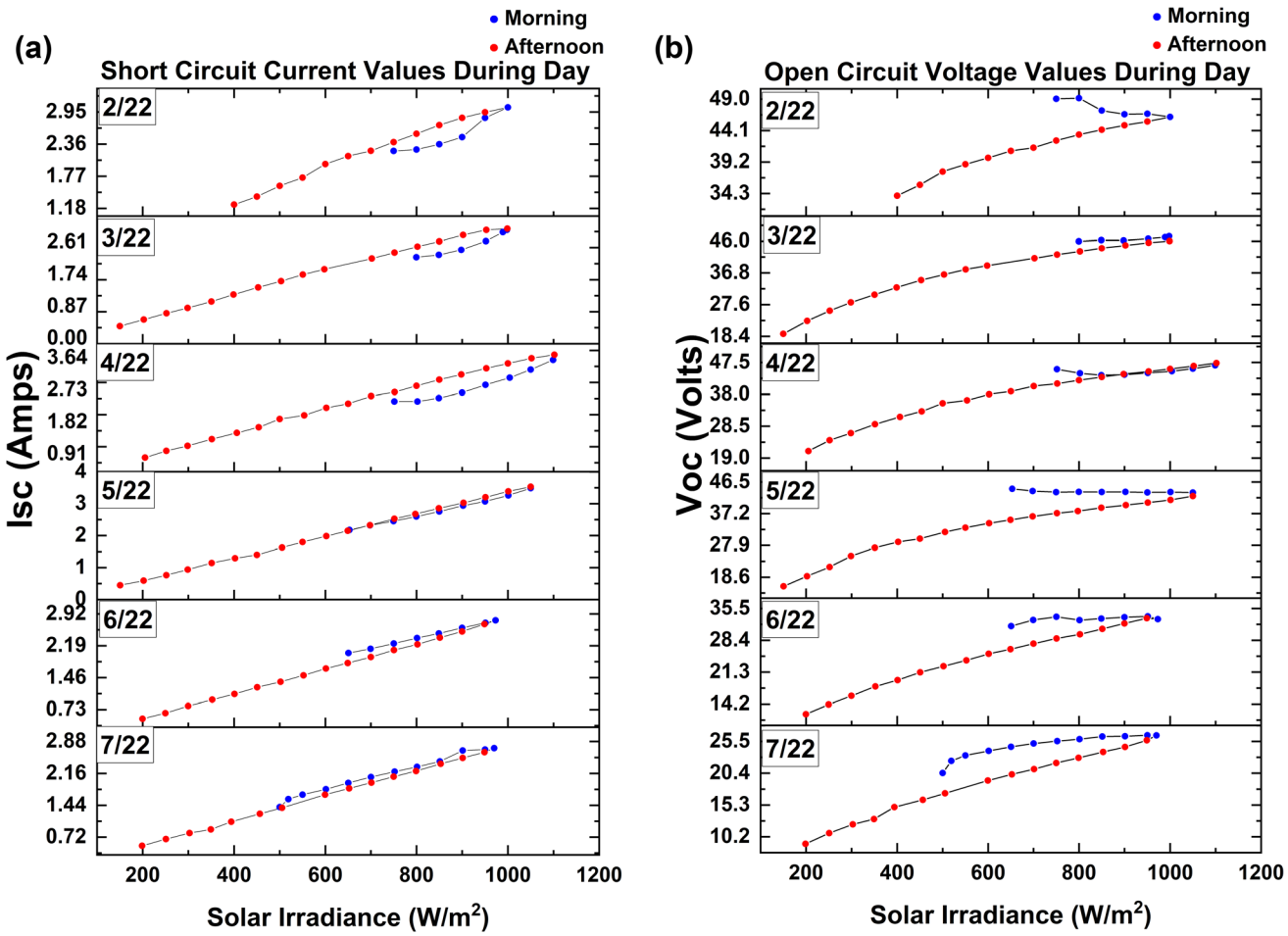

Fig. 8 . Evidence of the light soaking phenomenon affecting the electrical characteristics of the solar farm behavior charge during the day for each month after a 3-month dark storage period.

and the lamination failure on the overall production of the solar farm during LSP. Fig. 7 demonstrates that all electrical characteristics of panels #7 and #5 during LSP exhibit the same behavior. The results for the remaining GRAPE panels are shown in ESI Fig. 6.†

The data extracted from individual LSP measurements were analyzed, as shown in Fig. 7 and Table S4,† clearly indicating that the short-circuit current, maximum power, and efficiency of each panel follow the same trend as those of the open-circuit voltage.

The solar farm as a whole aligns with the majority of panels in terms of behavioral trends, showing an intermediate pattern. The effect of light soaking (LS) under 1000 W m^{-2} for 60 minutes before and after dark storage (DS) on the electrical performance of the perovskite panels was quantified. The observed variations in FF, P_{max}, I_{sc}, and V_{oc} are presented in Fig. 6 of the ESI,† where box charts illustrate the percentage (%) of open circuit voltage losses and gains associated with LS are presented in ESI Fig. 9.† A detailed quantitative analysis of these variations is provided in Tables S3 and S4 of the ESI.†

Diurnal variation per month after dark recovery

The difference between the morning and afternoon data of I_{sc} dependence on the illumination of the solar farm in a monthly analysis is plotted in Fig. 8, after the dark storage period (February 2022 to July 2022).

As reported in our previous study,[8] the V_{oc} values during the day appear to be reduced during the afternoon hours compared to the corresponding values in the morning at the same solar radiation. Regarding the differences between I_{sc} values recorded at the same solar irradiance in the afternoon and morning periods, no difference was observed since the light-induced degradation (LID)[26,27,34,43,44,79–85] effect had no direct effect on the production of the current at this time. By plotting (Fig. 8a) the corresponding morning-afternoon graphs after 3-month DS (months 5/22, 6/22, 7/22), we observed an abnormal behavior, consisting of an I_{sc} increase in the afternoon period compared with what we observed during the morning session at similar irradiance values. This confirms dark storage degradation and light recovery of some panels, as mentioned earlier, resulting in an increase in current. In contrast, the V_{oc} shows the same behavior, *i.e.*, in the afternoon, the V_{oc} values are always reduced (Fig. 8b) compared with the morning before and after DS. However, significant differences were observed in the first morning V_{oc} values (the voltage decreases despite the increase in irradiance) because they were strongly affected by the LSP effect each month.

As the panels are gradually restored and the behavior of the V_{oc} in the light soak changes, the same change appears in the V_{oc} values during the morning measurements. Finally, while the panels have regained the "ascending behavior" by comparing the V_{oc} values at the morning/afternoon transition, the same behavior is observed as well. Moreover, the I_{sc} behavior was restored to the original behavior, *i.e.*, the morning values should be the same in the afternoon for the corresponding solar irradiance values.

The measurement protocol effect, as well as the effect of LSP and LID on V_{oc} solar irradiance dependence, clearly indicate that the conventional, static MPP tracking algorithms used for commercial PV systems, such as fractional open circuit voltage MPP tracking,[86,87] are not suitable for perovskite photovoltaics and new algorithms should be introduced for more accurate MPP tracking[88] of this PV technology.

Two days experiment

To verify the different behaviors of the GRAPE panels after the DS periods (02/2022), *I–V* measurements were presented (ESI Fig. 3†) on all panels for two consecutive days to investigate the impact of LID[44,83,84] on the electrical properties of the panels. Some panels exhibited reduced electrical properties, as expected due to LID,[89] particularly affecting the V_{oc} and consequently the FF. Thus, the V_{oc} of all panels decreased on the second day.

However, the solar irradiance exposure had different effects on the current and maximum power in the two scenarios, as described in the following text and shown in Fig. 9.

In the first scenario, a subset of panels showed an increase in current after exposure to solar irradiance (ESI Fig. 3†). These panels had improved electrical properties on the second day, contributing to the observed increase in current. Additionally, the V_{oc} decreased, as expected, due to the effects of LID.[43,79,85] Thus, P_{max} increased because the increase in current was greater than the reduction in V_{oc}.

In the second scenario, a different subset of panels exhibited lower V_{oc}, I_{sc}, and P_{max} values after exposure to solar irradiance.

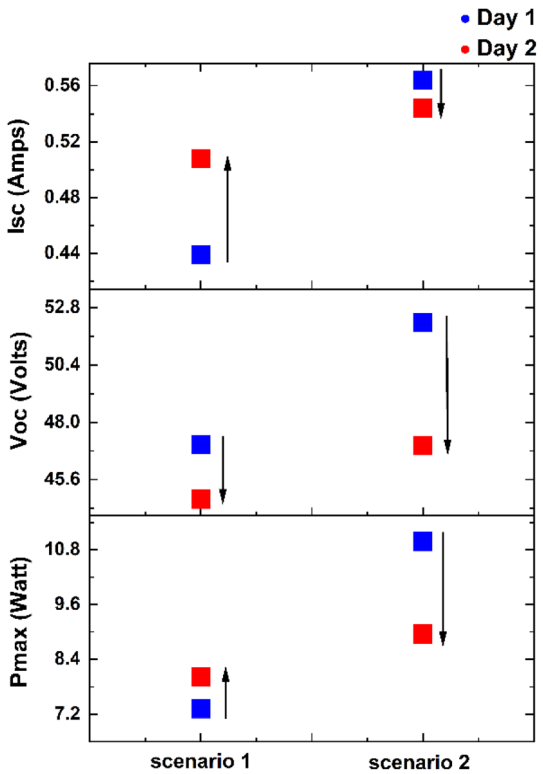

Fig. 9 Direct comparison of electrical characteristics for two consecutive days showcasing the two behavioral scenarios of the GRAPE panels.

These panels exhibit reduced electrical properties, which can be attributed to the impact of prolonged light exposure.

The findings from the two-day experiment once again validate that the behavior of perovskite photovoltaic cells, in relation to recovery phenomena, is closely linked to the level of degradation they are experiencing. Specifically, panels with degradation levels $>T_{50}$ recover in the dark, whereas those that are more degraded show a reduction in their characteristics during dark storage and then recover once exposed to light conditions.

This effect is caused by the ion-vacancy recombination process[36] enabled by photo-induced halide redistribution, which could lead to current modulation upon illumination mentioned earlier in this study and justifies the observed diurnal variations from the previous chapter, where short-circuit current values were higher in the afternoon compared to the morning, despite identical radiation intensity levels.

Conclusion

In summary, this study investigated the long-term performance of perovskite panels based on solar farms outdoors, with particular emphasis given to the origin of various degradation factors, some of which were intrinsic to the perovskite active layer, while others were extrinsic due to lamination failure. The detailed measurement protocols enabled an analysis of the effects of dark storage and light soaking on panels and partial recovery of the solar farm. The long-term stability of perovskite panels is a significant challenge due to the inherent sensitivity of perovskites to environmental conditions like humidity, high temperatures, and light exposure, which are degradation sources. The experimental findings of this study indicate a greater degradation of the solar farm during summer, resulting from prolonged exposure to high temperatures and solar irradiance, which has a severe effect on panel lamination stability. This degradation is partially reversible in dark storage. After the DS, not only was an improvement in the electrical parameters of the solar farm recorded, but also a different behavior in terms of the LSP was observed. Depending on the degradation level of the panels, different DS times were required to achieve sufficient recovery. Specifically, during the early stages of panel operation, recovery occurs in the day–night cycle; however, in later stages where stronger degradation appears, more time is needed for recovery. Notably, at very low degradation levels, the panels cannot restore their properties when simply stored in the dark; however, exposure to light illumination is required afterwards for performance recovery. This indicates that a complex interplay of degradation and recovery mechanisms exists that depends on light exposure and dark storage. Depending on the season and environmental conditions in the area where the GRAPE panels are installed, the electrical parameters can degrade slower or faster, as shown by the seasonal behavior of degradation. One potential real-world application of the dark recovery (DS) effect in perovskite solar panels is the implementation of periodic operational cycles to mitigate performance degradation. For instance, in installations where continuous energy production is not a priority, such as seasonal residences or off-grid applications with intermittent demand, panels could be periodically taken offline and covered to allow their electrical properties to recover before the next operational cycle. By strategically managing the exposure time to illumination and recovery periods, the long-term stability of perovskite-based photovoltaics can be significantly extended.

In addition, this study revealed visually inspected defects in the panels, which were monitored over time. These findings are associated with lamination failure and the penetration of oxygen and moisture, suggesting that they have a detrimental effect on perovskite solar farm performance. In the case of severe optical degradation, the electrical parameters of the corresponding panels cannot be restored even after being stored in the dark. Therefore, visual inspection during the panels' lifetime operated under outdoor conditions is an efficient way to identify the vulnerable points that occur either due to manufacturing dysfunctions or inherent material degradation, with the aim of technology optimization towards future designs. Identifying and preventing lamination failure and moisture penetration are critical for improving panel durability and stability while minimizing visual defects and ensuring optimal performance. This optimization strategy will contribute to the development of more reliable and durable perovskite solar panels, facilitating the widespread adoption of this promising renewable energy technology.

Another necessary step towards the commercialization of this photovoltaic technology is to study the voltage mismatch of perovskite photovoltaics to determine if and to what extent it affects their degradation rate. This, as well as their optimum connection configuration (parallel and in series), is used both in the upscaling process and in the fabrication of panels, as well as in the connection of panels for the most efficient long-term operation of a solar farm. Finally, we conclude that the lamination of the panels is the most important parameter for the stability of photovoltaic perovskites. From this study, we conclude that it is possible to restore the electrical properties of panels as long as the lamination prevents penetration of external parameters (oxygen and moisture) into the panels. However, additional studies on aging under outdoor conditions are necessary to differentiate the recovery scenarios in terms of their long-term stability and degree of degradation.

Data availability

The data that support the findings of this study are available in the ESI.†

Author contributions

E. S. contributed to the research conceptualisation and methodology, the execution of all experiments, the analysis of obtained data, the interpretation of the results, and the writing and visualisation of the initial manuscript draft. E. S., G. V. contributed to the research project conceptualisation and the experimental plan design. G. V., K. R., S. P., A. A., and N. T. contributed to the review and editing of the draft. E. S. and N. T. contributed to result analysis, mechanism discussion methodology, and editing. A. D. C. and E. K. provided resources,

contributed to data analyses and performed supervision. All authors revised and reviewed the manuscript.

Conflicts of interest

There are no conflicts to declare.

Acknowledgements

The work has been supported by the European Union's Horizon 2020 research and innovation programme Graphene Core3 under grant agreement number 881603. A. D. C. acknowledges the support of the RdS project 2022–2024 MASE (working agreement with ENEA).

References

1 J. Park, J. Kim, H. S. Yun, M. J. Paik, E. Noh, H. J. Mun, M. G. Kim, T. J. Shin and S. Il Seok, *Nature*, 2023, **616**, 724.
2 R. Azmi, D. S. Utomo, B. Vishal, S. Zhumagali, P. Dally, A. M. Risqi, A. Prasetio, E. Ugur, F. Cao, I. F. Imran, A. A. Said, A. R. Pininti, A. S. Subbiah, E. Aydin, C. Xiao, S. I. Seok and S. De Wolf, *Nature*, 2024, **628**, 93.
3 J. Kettle, M. Aghaei, S. Ahmad, A. Fairbrother, S. Irvine, J. J. Jacobsson, S. Kazim, V. Kazukauskas, D. Lamb, K. Lobato, G. A. Mousdis, G. Oreski, A. Reinders, J. Schmitz, P. Yilmaz and M. J. Theelen, *Prog. Photovoltaics Res. Appl.*, 2022, **30**, 1365.
4 P. Holzhey, M. Prettl, S. Collavini, N. L. Chang and M. Saliba, *Joule*, 2023, **7**, 257.
5 J. Suo, B. Yang, E. Mosconi, D. Bogachuk, T. A. S. Doherty, K. Frohna, D. J. Kubicki, F. Fu, Y. Kim, O. Er-Raji, T. Zhang, L. Baldinelli, L. Wagner, A. N. Tiwari, F. Gao, A. Hinsch, S. D. Stranks, F. De Angelis and A. Hagfeldt, *Nat. Energy*, 2024, **9**, 172.
6 M. V. Khenkin, E. A. Katz, A. Abate, G. Bardizza, J. J. Berry, C. Brabec, F. Brunetti, V. Bulović, Q. Burlingame, A. Di Carlo, R. Cheacharoen, Y. B. Cheng, A. Colsmann, S. Cros, K. Domanski, M. Dusza, C. J. Fell, S. R. Forrest, Y. Galagan, D. Di Girolamo, M. Grätzel, A. Hagfeldt, E. von Hauff, H. Hoppe, J. Kettle, H. Köbler, M. S. Leite, S. (Frank) Liu, Y. L. Loo, J. M. Luther, C. Q. Ma, M. Madsen, M. Manceau, M. Matheron, M. McGehee, R. Meitzner, M. K. Nazeeruddin, A. F. Nogueira, Ç. Odabaşı, A. Osherov, N. G. Park, M. O. Reese, F. De Rossi, M. Saliba, U. S. Schubert, H. J. Snaith, S. D. Stranks, W. Tress, P. A. Troshin, V. Turkovic, S. Veenstra, I. Visoly-Fisher, A. Walsh, T. Watson, H. Xie, R. Yıldırım, S. M. Zakeeruddin, K. Zhu and M. Lira-Cantu, *Nat. Energy*, 2020, **5**, 35.
7 C. Polyzoidis, K. Rogdakis and E. Kymakis, *Adv. Energy Mater.*, 2021, **11**, 2101854.
8 S. Pescetelli, A. Agresti, G. Viskadouros, S. Razza, K. Rogdakis, I. Kalogerakis, E. Spiliarotis, E. Leonardi, P. Mariani, L. Sorbello, M. Pierro, C. Cornaro, S. Bellani, L. Najafi, B. Martín-García, A. E. Del Rio Castillo, R. Oropesa-Nuñez, M. Prato, S. Maranghi, M. L. Parisi, A. Sinicropi, R. Basosi, F. Bonaccorso, E. Kymakis and A. Di Carlo, *Nat. Energy*, 2022, **7**, 597.
9 V. Paraskeva, M. Hadjipanayi, M. Norton, A. Aguirre, A. Hadipour, W. Song, T. Fontanot, S. Christiansen, R. Ebner and G. E. Georghiou, *Energies*, 2023, **16**, 2608.
10 M. Khenkin, H. Köbler, M. Remec, R. Roy, U. Erdil, J. Li, N. Phung, G. Adwan, G. Paramasivam, Q. Emery, E. Unger, R. Schlatmann, C. Ulbrich and A. Abate, *Energy Environ. Sci.*, 2024, **17**, 602.
11 Q. Jiang, R. Tirawat, R. A. Kerner, E. A. Gaulding, Y. Xian, X. Wang, J. M. Newkirk, Y. Yan, J. J. Berry and K. Zhu, *Nature*, 2023, **623**, 313.
12 M. U. Ali, H. Mo, Y. Li and A. B. Djurišić, *APL Energy*, 2023, **1**, 020903.
13 M. Peplow, *Nature*, 2023, **623**, 902.
14 C. Liu, Y. Yang, H. Chen, J. Xu, A. Liu, A. S. R. Bati, H. Zhu, L. Grater, S. S. Hadke, C. Huang, V. K. Sangwan, T. Cai, D. Shin, L. X. Chen, M. C. Hersam, C. A. Mirkin, B. Chen, M. G. Kanatzidis and E. H. Sargent, *Science*, 2023, **382**, 810.
15 A. Agresti, S. Pescetelli, E. Magliano, G. Bengasi, C. Connelli, C. Gerardi, H. Pazniak, F. Bonaccorso, M. Foti and A. Di Carlo, *IEEE J. Photovoltaics*, 2022, **12**, 1273.
16 S. Bellani, A. Bartolotta, A. Agresti, G. Calogero, G. Grancini, A. Di Carlo, E. Kymakis and F. Bonaccorso, *Chem. Soc. Rev.*, 2021, **50**, 11870.
17 Best Research-Cell Efficiency Chart, can be found under **https://www.nrel.gov/pv/cell-efficiency.html**.
18 M. V. Khenkin, K. M. Anoop, I. Visoly-Fisher, Y. Galagan, F. Di Giacomo, B. R. Patil, G. Sherafatipour, V. Turkovic, H.-G. Rubahn, M. Madsen, T. Merckx, G. Uytterhoeven, J. P. A. Bastos, T. Aernouts, F. Brunetti, M. Lira-Cantu and E. A. Katz, *Energy Environ. Sci.*, 2018, **11**, 739.
19 A. Senocrate, T. Acartürk, G. Y. Kim, R. Merkle, U. Starke, M. Grätzel and J. Maier, *J. Mater. Chem. A*, 2018, **6**, 10847.
20 Y. Han, S. Meyer, Y. Dkhissi, K. Weber, J. M. Pringle, U. Bach, L. Spiccia and Y. B. Cheng, *J. Mater. Chem. A*, 2015, **3**, 8139.
21 A. K. Mishra and R. K. Shukla, *Mater. Today: Proc.*, 2019, **29**, 836.
22 M. Wang, W. L. Yim, P. Liao and Y. Shen, *ChemistrySelect*, 2017, **2**, 4469.
23 H. Zhang, X. Qiao, Y. Shen and M. Wang, *J. Energy Chem.*, 2015, **24**, 729.
24 S. Aharon, A. Dymshits, A. Rotem and L. Etgar, *J. Mater. Chem. A*, 2015, **3**, 9171.
25 G. Li, Z. Su, M. Li, H. K. H. Lee, R. Datt, D. Hughes, C. Wang, M. Flatken, H. Köbler, J. J. Jerónimo-Rendon, R. Roy, F. Yang, J. Pascual, Z. Li, W. C. Tsoi, X. Gao, Z. Wang, M. Saliba and A. Abate, *Adv. Energy Mater.*, 2022, **12**, 2202887.
26 Y. Liu, C. Xie, W. Tan, X. Liu, Y. Yuan, Q. Xie, Y. Li and Y. Gao, *Org. Electron.*, 2019, **71**, 123.
27 S.-W. Lee, S. Kim, S. Bae, K. Cho, T. Chung, L. E. Mundt, S. Lee, S. Park, H. Park, M. C. Schubert, S. W. Glunz, Y. Ko, Y. Jun, Y. Kang, H.-S. Lee and D. Kim, *Sci. Rep.*, 2016, **6**, 38150.
28 K. Domanski, B. Roose, T. Matsui, M. Saliba, S. H. Turren-Cruz, J. P. Correa-Baena, C. R. Carmona, G. Richardson,

J. M. Foster, F. De Angelis, J. M. Ball, A. Petrozza, N. Mine, M. K. Nazeeruddin, W. Tress, M. Grätzel, U. Steiner, A. Hagfeldt and A. Abate, *Energy Environ. Sci.*, 2017, **10**, 604.

29 M. O. Reese, S. A. Gevorgyan, M. Jørgensen, E. Bundgaard, S. R. Kurtz, D. S. Ginley, D. C. Olson, M. T. Lloyd, P. Morvillo, E. A. Katz, A. Elschner, O. Haillant, T. R. Currier, V. Shrotriya, M. Hermenau, M. Riede, K. R. Kirov, G. Trimmel, T. Rath, O. Inganäs, F. Zhang, M. Andersson, K. Tvingstedt, M. Lira-Cantu, D. Laird, C. McGuiness, S. (Jimmy) Gowrisanker, M. Pannone, M. Xiao, J. Hauch, R. Steim, D. M. DeLongchamp, R. Rösch, H. Hoppe, N. Espinosa, A. Urbina, G. Yaman-Uzunoglu, J.-B. Bonekamp, A. J. J. M. Van Breemen, C. Girotto, E. Voroshazi and F. C. Krebs, *Sol. Energy Mater. Sol. Cells*, 2011, **95**, 1253.

30 T.-Y. Yang, N. J. Jeon, H.-W. Shin, S. S. Shin, Y. Y. Kim and J. Seo, *Adv. Sci.*, 2019, **6**, 1900528.

31 R. G. Balakrishna, S. M. Kobosko and P. V. Kamat, *ACS Energy Lett.*, 2018, **3**, 2267.

32 N. E. Courtier, J. M. Cave, J. M. Foster, A. B. Walker and G. Richardson, *Energy Environ. Sci.*, 2019, **12**, 396.

33 W. Xiang, S. Liu and W. Tress, *Energy Environ. Sci.*, 2021, **14**, 2090.

34 W. Nie, J.-C. Blancon, A. J. Neukirch, K. Appavoo, H. Tsai, M. Chhowalla, M. A. Alam, M. Y. Sfeir, C. Katan, J. Even, S. Tretiak, J. J. Crochet, G. Gupta and A. D. Mohite, *Nat. Commun.*, 2016, **7**, 11574.

35 C. Zhao, B. Chen, X. Qiao, L. Luan, K. Lu and B. Hu, *Adv. Energy Mater.*, 2015, **5**, 1500279.

36 M. V. Khenkin, A. K. M., I. Visoly-Fisher, S. Kolusheva, Y. Galagan, F. Di Giacomo, O. Vukovic, B. R. Patil, G. Sherafatipour, V. Turkovic, H.-G. Rubahn, M. Madsen, A. V. Mazanik and E. A. Katz, *ACS Appl. Energy Mater.*, 2018, **1**, 799.

37 E. Velilla, F. Jaramillo and I. Mora-Seró, *Nat. Energy*, 2021, **6**, 54.

38 K. Tvingstedt, L. Gil-Escrig, C. Momblona, P. Rieder, D. Kiermasch, M. Sessolo, A. Baumann, H. J. Bolink and V. Dyakonov, *ACS Energy Lett.*, 2017, **2**, 424.

39 D. B. Khadka, Y. Shirai, M. Yanagida and K. Miyano, *ACS Appl. Energy Mater.*, 2021, **4**, 11121.

40 W. Tress, K. Domanski, B. Carlsen, A. Agarwalla, E. A. Alharbi, M. Graetzel and A. Hagfeldt, *Nat. Energy*, 2019, **4**, 568.

41 W. Song, X. Zhang, S. Lammar, W. Qiu, Y. Kuang, B. Ruttens, J. D'Haen, I. Vaesen, T. Conard, Y. Abdulraheem, T. Aernouts, Y. Zhan and J. Poortmans, *ACS Appl. Mater. Interfaces*, 2022, **14**, 27922.

42 K. Domanski, E. A. Alharbi, A. Hagfeldt, M. Grätzel and W. Tress, *Nat. Energy*, 2018, **3**, 61.

43 H. Shahivandi, M. Vaezzadeh and M. Saeidi, *Sol. Energy Mater. Sol. Cells*, 2020, **218**, 110770.

44 T. Duong, Y. L. Wu, H. Shen, J. Peng, S. Zhao, N. Wu, M. Lockrey, T. White, K. Weber and K. Catchpole, *Sol. Energy Mater. Sol. Cells*, 2018, **188**, 27.

45 K. M. Anoop, M. V. Khenkin, F. Di Giacomo, Y. Galagan, S. Rahmany, L. Etgar, E. A. Katz and I. Visoly-Fisher, *Sol. RRL*, 2020, **4**, 1900335.

46 G. Divitini, S. Cacovich, F. Matteocci, L. Cinà, A. Di Carlo and C. Ducati, *Nat. Energy*, 2016, **1**, 15012.

47 T. J. Silverman, M. G. Deceglie, I. R. Repins, T. Zhu, Z. Song, M. J. Heben, Y. Yan, C. Fei, J. Huang and L. T. Schelhas, *IEEE J. Photovoltaics*, 2023, **13**, 740.

48 S. Tan, T. Huang, I. Yavuz, R. Wang, T. W. Yoon, M. Xu, Q. Xing, K. Park, D. K. Lee, C. H. Chen, R. Zheng, T. Yoon, Y. Zhao, H. C. Wang, D. Meng, J. Xue, Y. J. Song, X. Pan, N. G. Park, J. W. Lee and Y. Yang, *Nature*, 2022, **605**, 268.

49 T. S. Ripolles, A. K. Baranwal, K. Nishinaka, Y. Ogomi, G. Garcia-Belmonte and S. Hayase, *Phys. Chem. Chem. Phys.*, 2016, **18**, 14970.

50 F. Huang, L. Jiang, A. R. Pascoe, Y. Yan, U. Bach, L. Spiccia and Y.-B. Cheng, *Nano Energy*, 2016, **27**, 509.

51 X. Zheng, J. Troughton, N. Gasparini, Y. Lin, M. Wei, Y. Hou, J. Liu, K. Song, Z. Chen, C. Yang, B. Turedi, A. Y. Alsalloum, J. Pan, J. Chen, A. A. Zhumekenov, T. D. Anthopoulos, Y. Han, D. Baran, O. F. Mohammed, E. H. Sargent and O. M. Bakr, *Joule*, 2019, **3**, 1963.

52 E. A. Gaulding, A. E. Louks, M. Yang, R. Tirawat, M. J. Wilson, L. K. Shaw, T. J. Silverman, J. M. Luther, A. F. Palmstrom, J. J. Berry and M. O. Reese, *ACS Energy Lett.*, 2022, **7**, 2641.

53 S. N. Laboratories N. Technology E. Solutions, *PACT Perovskite PV Module Outdoor Test Protocol V.0.1*, 2023.

54 C. X. Zhang, T. Shen, D. Guo, L. M. Tang, K. Yang and H. X. Deng, *InfoMat*, 2020, **2**, 1034.

55 D. Strachala, M. Kratochvíl, J. Hylský, A. Gajdoš, L. Chladil, J. Vaněk and P. Čudek, Development of Stable Perovskite Solar Cell, in *Renewable Energy Sources: Engineering, Technology, Innovation*, ed. M. Wróbel, M. Jewiarz and A. Szlęk, Springer Proceedings in Energy, Springer, Cham, 2020, pp. 653–655.

56 A. D. Sheikh, R. Munir, M. A. Haque, A. Bera, W. Hu, P. Shaikh, A. Amassian and T. Wu, *ACS Appl. Mater. Interfaces*, 2017, **9**, 35018.

57 A. F. Akbulatov, L. A. Frolova, N. N. Dremova, I. Zhidkov, V. M. Martynenko, S. A. Tsarev, S. Y. Luchkin, E. Z. Kurmaev, S. M. Aldoshin, K. J. Stevenson and P. A. Troshin, *J. Phys. Chem. Lett.*, 2020, **11**, 333.

58 Y. Guo, X. Yin, D. Liu, J. Liu, C. Zhang, H. Xie, Y. Yang and W. Que, *ACS Energy Lett.*, 2021, **6**, 2502.

59 M. Jošt, B. Lipovšek, B. Glažar, A. Al-Ashouri, K. Brecl, G. Matič, A. Magomedov, V. Getautis, M. Topič and S. Albrecht, *Adv. Energy Mater.*, 2020, **10**, 2000454.

60 A. D. Dhass, N. Beemkumar, S. Harikrishnan and H. M. Ali, *Int. J. Photoenergy*, 2022, 2986004.

61 K. A. K. Niazi, Y. Yang and D. Sera, *IET Renewable Power Gener.*, 2019, **13**, 2035.

62 O. Hentz, P. Rekemeyer and S. Gradečak, *Adv. Energy Mater.*, 2018, **8**, 1701378.

63 L. Flannery, J. Ogle, D. Powell, C. Tassone and L. Whittaker-Brooks, *J. Mater. Chem. A*, 2020, **8**, 25109.

64 R. A. Z. Razera, D. A. Jacobs, F. Fu, P. Fiala, M. Dussouillez, F. Sahli, T. C. J. Yang, L. Ding, A. Walter, A. F. Feil, H. I. Boudinov, S. Nicolay, C. Ballif and Q. Jeangros, *J. Mater. Chem. A*, 2020, **8**, 242.
65 L. Najafi, S. Bellani, L. Gabatel, M. I. Zappia, A. Di Carlo and F. Bonaccorso, *ACS Appl. Energy Mater.*, 2022, **5**, 1378.
66 D. A. R. Barkhouse, O. Gunawan, T. Gokmen, T. K. Todorov and D. B. Mitzi, *Prog. Photovoltaics Res. Appl.*, 2015, **20**, 6.
67 A. Rizzo, L. Ortolan, S. Murrone, L. Torto, M. Barbato, N. Wrachien, A. Cester, F. Matteocci and A. Di Carlo, in *IEEE International Reliability Physics Symposium Proceedings*, Institute Of Electrical And Electronics Engineers Inc., 2017, pp. PV1.1–PV1.6.
68 X. Deng, X. Wen, J. Zheng, T. Young, C. F. J. Lau, J. Kim, M. Green, S. Huang and A. Ho-Baillie, *Nano Energy*, 2018, **46**, 356.
69 L. Lin, L. Yang, G. Du, X. Li, Y. Li, J. Deng, K. Wei and J. Zhang, *ACS Appl. Energy Mater.*, 2023, **6**, 10303.
70 J. Hu, R. Gottesman, L. Gouda, A. Kama, M. Priel, S. Tirosh, J. Bisquert and A. Zaban, *ACS Energy Lett.*, 2017, **2**, 950.
71 S. Shao and M. A. Loi, *Adv. Mater. Interfaces*, 2020, **7**, 1901469.
72 K. Domanski, J. P. Correa-Baena, N. Mine, M. K. Nazeeruddin, A. Abate, M. Saliba, W. Tress, A. Hagfeldt and M. Grätzel, *ACS Nano*, 2016, **10**, 6306.
73 S. Mahesh, J. M. Ball, R. D. J. Oliver, D. P. McMeekin, P. K. Nayak, M. B. Johnston and H. J. Snaith, *Energy Environ. Sci.*, 2020, **13**, 258.
74 K. Yao, S. Li, Z. Liu, Y. Ying, P. Dvořák, L. Fei, T. Šikola, H. Huang, P. Nordlander, A. K.-Y. Jen and D. Lei, *Light Sci. Appl.*, 2021, **10**, 219.
75 D. B. Khadka, Y. Shirai, M. Yanagida and K. Miyano, *J. Mater. Chem. C*, 2018, **6**, 162.
76 M. R. Khan, J. A. Schwenzer, J. Lehr, U. W. Paetzold and U. Lemmer, *J. Phys. Chem. Lett.*, 2022, **13**, 552.
77 S. R. Raga and Y. Qi, *J. Phys. Chem. C*, 2016, **120**, 28519.
78 E. Von Hauff and D. Klotz, *J. Mater. Chem. C*, 2022, **10**, 742.
79 A. Farooq, M. R. Khan, T. Abzieher, A. Voigt, D. C. Lupascu, U. Lemmer, B. S. Richards and U. W. Paetzold, *ACS Appl. Energy Mater.*, 2021, **4**, 3083.
80 J. Lim, M. Kim, H. H. Park, H. Jung, S. Lim, X. Hao, E. Choi, S. Park, M. Lee, Z. Liu, M. A. Green, J. Seo, J. Park and J. S. Yun, *Sol. Energy Mater. Sol. Cells*, 2021, **219**, 110776.
81 V. Stoichkov, N. Bristow, J. Troughton, F. De Rossi, T. M. Watson and J. Kettle, *Sol. Energy*, 2018, **170**, 549.
82 E. Kobayashi, R. Tsuji, D. Martineau, A. Hinsch and S. Ito, *Cell Rep. Phys. Sci.*, 2021, **2**, 100648.
83 J. P. Bastos, U. W. Paetzold, R. Gehlhaar, W. Qiu, D. Cheyns, S. Surana, V. Spampinato, T. Aernouts and J. Poortmans, *Adv. Energy Mater.*, 2018, **8**, 1800554.
84 P. H. Joshi, L. Zhang, I. M. Hossain, H. A. Abbas, R. Kottokkaran, S. P. Nehra, M. Dhaka, M. Noack and V. L. Dalal, *AIP Adv.*, 2016, **6**, 115114.
85 S. J. Yoon, M. Kuno and P. V. Kamat, *ACS Energy Lett.*, 2017, **2**, 1507.
86 A. Hmidet, U. Subramaniam, R. M. Elavarasan, K. Raju, M. Diaz, N. Das, K. Mehmood, A. Karthick, M. Muhibbullah and O. Boubaker, *Int. J. Photoenergy*, 2021, **2021**, 4925433.
87 T.-W. Hsu, H.-H. Wu, D.-L. Tsai and C.-L. Wei, *IEEE Trans. Circuits Syst. II Express Briefs*, 2019, **66**, 25.
88 A. F. Murtaza, H. A. Sher, M. Chiaberge, D. Boero, M. De Giuseppe and K. E. Addoweesh, *Proceedings of 15th International Conference on Mechatronics*, MECHATRONIKA, 2012 2012, vol. 1.
89 N. Rolston, R. Bennett-Kennett, L. T. Schelhas, J. M. Luther, J. A. Christians, J. J. Berry and R. H. Dauskardt, *Science*, 2020, **368**, eaay8691.